



Comparison of Secondary Electron Emission simulation to experiment

Z. Insepov^{a*}, V. Ivanov^b, S. J. Jokela^a, I. Veryovkin^a, A. Zinovev^a, and H. Frisch^c

^a Argonne National Lab., 9700 S. Cass Avenue, Argonne, IL 60439, USA

^b Muons, Inc., 552 N. Batavia Ave., Batavia, IL 60610, USA

^c High-Energy Physics Division, Argonne National Laboratory, Argonne, Illinois

Elsevier use only: Received date here; revised date here; accepted date here

Abstract

The secondary electron emission (SEE) yields were calculated for various materials and a good comparison has been obtained with the experimental data for gold measured at ANL. The calculation method uses Monte Carlo simulation, empirical theories, and close comparison to experiment, in order to parameterize the SEE yields of highly emissive materials for microchannel plates. The simulation results will be used in the selection of emissive and resistive materials for the deposition and characterization experiments that will be conducted by a large-area fast detector project at Argonne National Laboratory

© 2008 Elsevier Science. All rights reserved

PACS: 29.40.Ka; 79.20.Hx; 61.43.Bn.

Keywords: Secondary electron emission; Monte Carlo simulation; gold;

1. Introduction

Theoretical models of secondary electron emission (SEE) yields for highly emissive materials are

important for development of particle detectors for high-energy physics, such as Cherenkov, neutrino, and astroparticle detectors, scanning electron microscopy (SEM) development [1-4,7-15].

In this work, a parameterized set of the SEE-yield dependencies on two variables, the primary electron

* Corresponding author. Tel.: +1-630-252-5049; fax: +1-630-252-5049; e-mail: insepov@anl.gov.

energy (E_{PE}) and the angle of incident electrons (θ), is compared to the experimental data obtained for several highly emissive materials of interest for the large-area fast detector development.

The calculations will be verified with the experimental data for gold as a reference material, specifically measured for the large-area fast detector project. The calculated yields will be mainly used as input files for macroscopic MCP gain and transient time calculation codes for computing electron trajectories inside MCPs of various types, such as chevron and funnel. Feedback from the gain code will then be used to improve the materials data and will stimulate further search for the best MCP emissive and resistive materials.

2. Secondary electron emission yields

Several semi-empirical theories were developed regarding electron yield [7-13]. These theories are helpful in calibrating Monte Carlo simulations, which are the main tool for obtaining the SEE yield for various materials at different energies and incident angles of primary electrons. Specifically, if no reliable theoretical or experimental data for the parameters of secondary emission yields, such data can be obtained from Monte Carlo simulations and be used to quantify the SEE yields for new materials by using the empirical laws. An extensive analysis has been done by Lin and Joy [8], who obtained a universal law for 44 elements with $Z = 3-83$.

Several researchers have developed Monte Carlo codes based on the above theory that are applicable to low-energy SEE-yield calculations [3,4,7-9]. The Rutherford cross-section for elastic electron scattering of low-E electrons and high-Z materials was replaced by Mott's cross-section, which was tabulated for the electron energies in the range of 1-100 keV [3]. The inelastic energy loss of electrons is usually approximated by Bethe's equation.

Berger and Seltzer [9] proposed an empirical formula applicable to high-energy electrons as follows:

The Bethe approximation (10) was improved by Seiler [12] for low-energy electrons. Two important simulation parameters are used in the Monte Carlo model. One is ϵ , the average energy for producing

secondary electron, and the other is the escape depth λ . These two parameters have a significant impact on the simulation result. We used $\epsilon = 20$ eV for Al_2O_3 [10]. The escape depth λ of insulators can be relatively large compared to that of metal surfaces, a direct effect of the small absorption coefficient of low-energy electrons in insulators because of the large energy band gap (e.g., $E_g = 8$ eV in Al_2O_3).

Kanaya et al. [11] proposed a theoretical model for calculating the escape depth for a range of insulators and alkaline materials. Based on this analysis, the escape length can be chosen as $\lambda = 60 \text{ \AA}$ for Al_2O_3 . This value was also suggested by Joy [10].

3. Simulation results

The simulation results for the electron energies above ~ 200 eV were obtained by using Monte Carlo codes developed in [3,4, 4-10]. A detailed explanation of the algorithm used in these codes can be found in [3,7]. For electrons with energies below ~ 200 eV, the inelastic energy loss was modified according to the algorithm proposed by Joy [9]. For electron energies below 50 eV, we used the "universal law of SEE yield" given by in [8].

The main adjustable parameters of the Monte Carlo simulations are the escape length λ and the average energy per secondary electron emission ϵ that were used in eq. (6) [7-11]. The escape length of ZnO was used as an adjustable parameter. The following material's parameters were used: λ was varied between 40 for low- and 20 \AA for high-energy regions, according to a suggestion by Joy [9], and $\epsilon = 125$ eV [11]. These parameters are listed in Table 1.

Material parameters

Material	ϵ , eV	λ , \AA
Al_2O_3	20 [9]	60 [10]
MgO	20 [11]	120 [11]
ZnO	125 [11]	30 [this work]
Gold	40 [8]	7 [8]

4. Comparison with experiment

Since the charging of highly resistive ceramics gives incorrect SEE-yield results, it is important to

compare the experimental measurements with the Al_2O_3 emission rates obtained by Monte Carlo simulations. Our result shows close agreement between experiment [21] and our simulation.

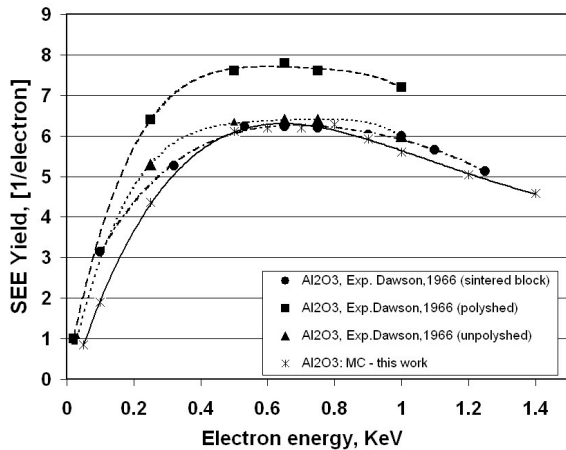


Figure 1. Comparison of our results calculated by Monte Carlo method for Al_2O_3 with experimental data obtained in [21] for polished (squares and dashed line), unpolished (triangles and dotted line), and sintered surface (circles and dash-dotted) curves and symbols. Our simulation is shown as stars symbols and fitted by solid curve..

MC simulations were also conducted for the SEE yields of ZnO samples, and the results of our simulations were compared with the experimental results by Gornyi [22]. The agreement between the simulated and measured data is close at the maximum of SEE yield but less comparable at the low energy end. Our MC results were also compared with MgO data measured in [23-25].

A detailed study of SEE were carried out for gold, since this material was chosen as a reference for our secondary electron emission experiments.

Our experimental setup uses the electron gun from a Low Energy Electron Diffraction (LEED) system as an electron source of fixed energy, 850eV for this experiment. The kinetic energy of the electrons is varied by applying a negative potential to the sample using a Keithley Source Meter, which also samples the electrical current flow. The initial beam current, I_{beam} , is sampled by applying a positive 1100 volt bias to the sample, preventing all secondary electrons from escaping the sample. We then vary the sample voltage from -850V to 0V in one volt increments,

measuring the current flow at every point. The gain, γ , is then calculated using the following equation

$$\gamma = \frac{I_{collector}}{I_{beam}} = 1 - \frac{I_{sample}}{I_{beam}}, \quad (1)$$

where instead of using an external collector to collect the secondary electrons, we simply measure the current flowing from the voltage source used to bias the sample, I_{sample} .

This system is included in an ultra-high vacuum chamber (4×10^{-10} torr) along with a 5 keV Ar ion source for sputter cleaning and an X-ray Photoelectron Spectrometer (XPS) which uses an Mg K-alpha x-ray source (1253 eV) and a hemispherical electron energy analyzer (HA100 from VSW Scientific Instruments). The x-ray beam is neither collimated nor passed through a monochromator. However, the x-ray emission is narrow enough to obtain compositional information as well as some chemical information from samples. This system also includes a helium UV source for use in Ultraviolet Photoelectron Spectroscopy (UPS) which will be used in the future to better relate band structure with surface composition and how they tie into the secondary electron emission of a broad range of materials.

Our analysis of gold showed a strong correlation between surface composition/cleanliness and secondary electron emission. The gold foil sample used in this study was stored on shelf and had an unknown history. Sample composition and secondary electron yield as a function of incident electron energy was measured before and after 5keV Ar^+ sputter cleaning. Before Ar-ion cleaning, we observe a strong carbon and oxygen contamination, most likely from surface contamination accumulated during the storage of the sample.

The secondary yield from this sample was much lower than expected for clean gold (Fig. 2). It is suspected that the surface contamination provides an extra barrier for secondaries escaping the surface. This layer may also provide some secondary electrons as the primary electrons pass through. After Ar-ion cleaning, we see the near-elimination of carbon and oxygen contamination. There also appears to be an increase in Si from an unknown source. It's possible this Si is an impurity in the gold foil. We also see an increase in secondary electron yield (Fig.

2). This shows that even a small amount of contamination on the surface greatly affects the secondary yield of a sample.

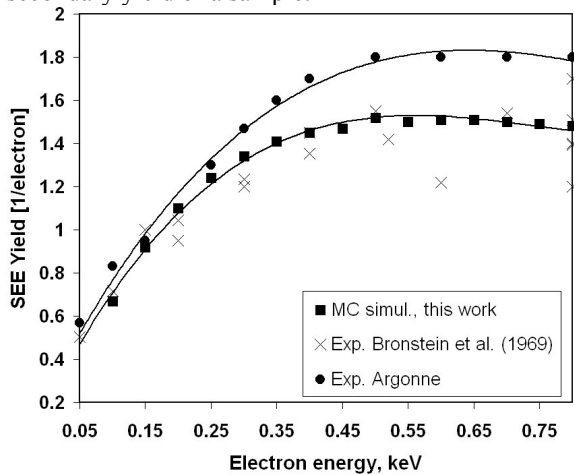


Fig. 2. Secondary electron yield for gold foil measured in this work after 30 minutes Ar-ion sputter cleaning (solid circles) and in experiment [26] (crosses) compared with our calculations (solid squares).

Acknowledgments

We thank D. Joy and P. Hovington for sharing their codes and giving valuable suggestions for the simulation parameters.

This work was supported by the U.S. Department of Energy, under Contract DE-AC02-06CH11357.

References

- [1] E. Nappi, Advances in the photodetection technologies for Cherenkov imaging applications, *Nucl. Instr. Meth. A* 604 (2009) 190-192.
- [2] S.M. Bradbury, R. Mirzoyan, J. Gebauer, E. Feigl, E. Lorenz, Test of the new hybrid INTEVAC intensified photocell for the use in air Cherenkov telescopes, *Nucl. Instr. Meth. A* 387 (1997) 45-49.
- [3] L. Reimer, D. Stelter, FORTRAN 77 Monte-Carlo program for minicomputers using Mott cross-section, *Scanning* 8 (1986) 265-277.
- [4] S. Ishimura, M. Aramata, R. Shimizu, Monte-Carlo calculation approach to quantitative Auger electron spectroscopy, *J. Appl. Phys.* 51 (1980) 2853-2860.
- [5] D.R. Beaulieu, D. Gorelikov, P. de Rouffignac, K. Saadatmand, K. Stenton, N. Sullivan, and A.S. Tremsin, Novel microchannel plate device fabricated with atomic layer deposition, AVS Topical Conf. on Atomic Layer Deposition, ALD 2009, Monterey, CA, July 19-22, 2009.
- [6] J.A. Anderson¹, K. Byrum¹, G. Drake¹, C. Ertley, H. Frisch, J.-F. Genat, E. May, D. Salek, F. Tang, New developments in fast-sampling analog readout of MCP based large-area picosecond time-of-flight detectors, *IEEE-MIC* 2008, ID-2973.
- [7] D.C. Joy, Monte Carlo modeling for electron microscopy and microanalysis, Oxford Univ. Press, 1995.
- [8] Y. Lin, D.C. Joy, A new examination of secondary electron yield data, *Surf. Interface Anal.* 37 (2005) pp. 895-900.
- [9] D.C. Joy, A model for calculating secondary and backscattering electron yields, *J. Microscopy*, 147 (1987) 51-64.
- [10] D.C. Joy, private communication, 2009.
- [11] K. Kanaya, S. Ono, F. Ishigaki, Secondary electron emission from insulators, *J. Phys. D* 11 (1978) 2425-2437.
- [12] H. Seiler, Secondary electron emission in the scanning electron microscope, *J. Appl. Phys.* 54 (1983) R1-R18.
- [13] J.R. Young, Penetration of electrons in Al₂O₃-films, *Phys. Rev.* 103 (1956) 292-293.
- [14] R.O. Lane, D.I. Zaffarano, Transmission of 0-40 keV electrons by thin films with application to beta-ray spectroscopy, *Phys. Rev.* 94 (1954) 960-964.
- [15] K. Ohya, I. Mori, Influence of backscattered particles on angular dependence of secondary electron emission from Copper, *J. Phys. Soc. Jpn.* 59 (1990) 1506-1517.
- [16] M. Ito, H. Kume, K. Oba, Computer analysis of the timing properties in micro channel plate photomultiplier tubes, *IEEE Trans. NS-31* (1984) 408-412.
- [17] A.J. Guest, A computer model of channel multiplier plate performance, *Acta Electronica*, 14 (1971) pp.79-97.
- [18] M. Baroody, A theory of secondary electron emission from metals, *Phys. Rev.* 78 (1950) 780-787.
- [19] P.H. Dawson, Secondary electron emission yields of some ceramics, *J. Appl. Phys.* 37 (1966) 3644-3665.
- [20] N.B. Gornyi, Secondary electron emission for different faces of a Zn single crystal covered with crystalline zinc oxide films, *JETP* 26 (1954) pp. 88-97. (in Russian)
- [21] N.R. Whetten, A.B. Laponsky, Secondary electron emission of single crystals of MgO, *J. Appl. Phys.* 28 (1957) pp. 515-516.
- [22] Y. Ushio, T. Banno, N. Matuda, Y. Saito, S. Baba, A. Kinbara, Secondary electron emission studies on MgO films, *Thin Solid Films*, 167 (1988) pp. 299-308.
- [23] A.J. Dekker, Secondary electron emission, in *Solid State Phys.*, vol. 6, ed. F. Seitz, D. Turnbull, H. Ehrenreich. Academic Press, NY (1958) pp. 251-311.
- [24] I.M. Bronstein, B.S. Fraiman, eds., in "Vtorichnaya Elektronnaya Emissiya", (Nauka: Movkva), (1969) p. 340 (In Russian)

The submitted manuscript has been created by UChicago Argonne, LLC, Operator of Argonne National Laboratory ("Argonne"). Argonne, a U.S. Department of Energy Office of Science laboratory, is operated under Contract No. DE-AC02-06CH11357. The U.S. Government retains for itself, and others acting on its behalf, a paid-up nonexclusive, irrevocable worldwide license in said article to reproduce, prepare derivative works, distribute copies to the public, and perform publicly and display publicly, by or on behalf of the Government.